

Effect of Dislocations on Ultrasonic Wave Attenuation in Metals*

By W. P. MASON

(Manuscript received April 6, 1955)

The causes of energy dissipation and mechanical instabilities of the elastic constants in metals can usually be traced to the presence of an imperfection in the crystal lattice called a dislocation. Edge dislocations are regions in the lattice where an extra plane of atoms has been added or subtracted from an otherwise perfect crystal. Such dislocations can move through the crystal under the application of shearing stresses or because of thermal agitation. It is shown that the primary causes of energy dissipation in a metal are dislocation loops pinned at irregular intervals by impurity atoms. At very low temperatures these dislocations lie along minimum energy positions but at higher temperatures they can be displaced to the next minimum energy position. In going to the next position, the dislocation meets an energy barrier determined by the energy required to overcome the limiting shearing stress T_{130} and the energy to stretch the dislocation. This barrier causes a relaxation effect for which the dislocations lag behind the applied stress and abstract energy from the mechanical vibrations. By measuring the position and height of the relaxation peak as a function of frequency and temperature, evidence is obtained for the value of the limiting shearing stress, the number of dislocations per square cm., and the average loop length. The values obtained agree with other methods for measuring these quantities.

At higher temperatures thermal agitation causes the loops to break away from their pinning impurity atoms. In the process, it is shown that a loss occurs which is independent of frequency and amplitude but which varies exponentially with the temperature. The activation energy found agrees with the calculated value for the binding energy of an impurity atom. Dislocations also occur at the boundaries between grains in the metal and produce a peak in the measured attenuation of a polycrystal which reaches a maximum at high temperatures and low frequencies. The activation energy for this process is determined by the energy required for a vacancy to diffuse

* *Editor's Note:* The present paper is a chapter of a new book entitled "Ultrasonics in Solids", which is scheduled for publication by D. Van Nostrand in 1956.

from one position to another. This energy is somewhat less than the bulk diffusion energy on account of the strains in the grain boundary.

Highly worked metals show two other effects due to dislocations, called the Köster effect and the viscosity effect. It appears that these are due to zig zag dislocations which do not lie in minimum energy positions. In the course of time free dislocations become pinned and the Köster effect disappears.

INTRODUCTION

Metals are used very considerably in conducting sound waves in such applications as mechanical filters, reed relays, low frequency delay lines, and ultrasonic processing devices. In all of these devices, the energy loss and the stability of the elastic properties of the metals are of prime importance. The causes of energy losses and instabilities in all solid materials are associated with the molecular motions that can take place under thermal agitation and under the stresses that are applied to the materials. For metals, most of the irreversible processes have been interpreted in terms of a type of imperfection known as a dislocation. While it is not within the scope of this book to discuss dislocation theory in detail,¹ a short introduction is given in order to provide a background for the ultrasonic measurements discussed in this chapter.

Dislocations were first introduced into the theory of metals to explain the fact that the limiting shear stress required to cause plastic flow in very pure single crystals was such a small fraction of the shear elastic constant of the crystal. Various measurements for very pure metals have shown that the limiting shear stress may be only 1/60,000 times the elastic shear modulus μ at room temperature and not more than three times this value at absolute zero. Without invoking imperfections of some type it is very difficult² to explain why the limiting shearing stress

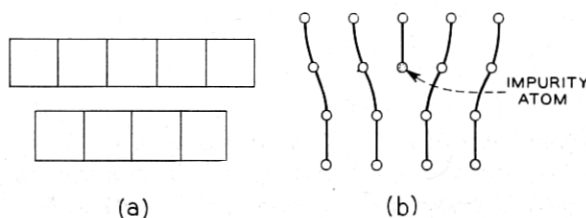


Fig. 1 — Edge dislocation showing position for small impurity atom.

¹ Complete discussions of dislocation theory have been given in two recent books, A. H. Cottrell, *Dislocations and Plastic Flow in Crystals*, Oxford University Press, 1953, and W. T. Read, *Dislocations in Crystals*, McGraw-Hill Company, 1953.

² See A. H. Cottrell, loc. cit., pp. 8-12.

should be less than $1/30$ of μ . A type of imperfection known as an edge dislocation was first introduced by G. I. Taylor and E. Orowan to explain this effect. An edge dislocation, as shown by Fig. 1, is a region in a crystal lattice where an extra row of atoms is either introduced or abstracted from an otherwise perfect crystal. This can be accommodated only if the crystal is severely strained in the joining region, with a high compression in the region of too many planes and a high tension in the region of too few planes.

Experiment has shown that these dislocations are mobile and move in close packed atomic planes since the energy they have to overcome in these planes is less than in other planes. For face centered metals such as aluminum, lead, copper, and silver this plane is the (111) plane which is the plane perpendicular to the cube diagonal as shown by Fig. 2. The direction of motion is in the $10\bar{1}$ direction which is the direction for which successive atoms are closest together. As can be seen from Fig. 2, the distance b that they are separated is $1/\sqrt{2}$ times the cube edge for the unit cell. Body-centered crystals glide along the (110) plane in the $[111]$ direction. Table I shows³ the number of glide planes, glide directions and atomic spacings for several types of crystal structures.

Returning to the problem of the limiting shearing stress, it is obvious

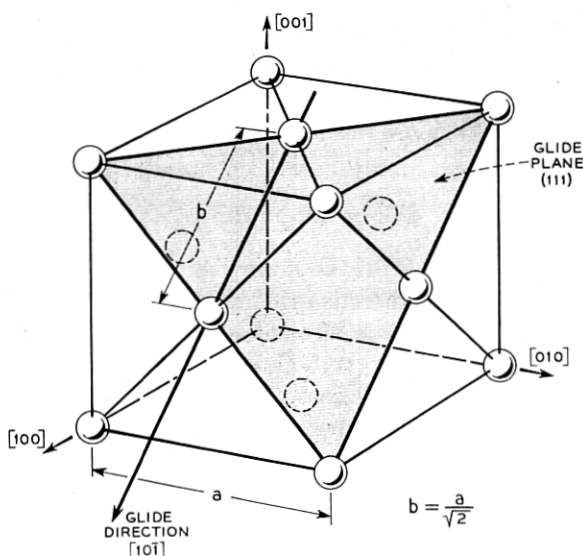


Fig. 2 — Glide plane, glide direction and glide distance b for a face centered metal.

³ See W. T. Read, loc. cit., p. 22.

TABLE I

Structure	Glide Plane	Glide Direction	Magnitude in terms of cube edge	Number of glide directions
Simple cubic.....	010	100	1	3
Face-centered cubic.....	111	110	$\frac{1}{\sqrt{2}}$	6
Body-centered cubic.....	110	111	$\frac{1}{2}\sqrt{3}$	4

that with this type of imperfection it will require less force to move a plane of atoms to the next minimum energy position one molecular distance b from the first minimum energy position. This follows from the fact that the large force required to push one atom by another one is partly cancelled by the attraction of the next atom for its opposite number on the other side of the dislocation. This force depends on the width of the dislocation, i.e., the number of atom planes over which the dislocation is spread. Various assumptions are considered by Cottrell⁴ who finds that the limiting shearing stress should be in the range

$$T_{13_0} = 4.0 \times 10^{-6} \mu \text{ to } 3.6 \times 10^{-4} \mu \quad (1)$$

As discussed in the next section, an ultrasonic relaxation at low temperatures has been found which correlates with the energy required to move a dislocation from one minimum energy position to the next one at a distance b from the first against the limiting shear stress T_{13_0} and it is found that

$$T_{13_0} \cong 6.0 \times 10^{-6} \mu, \quad (2)$$

in satisfactory agreement with the lower limit of (1).

In a pure single crystal there is evidence that the dislocations form a network which outlines mosaic blocks having slightly different orientations from each other in the crystal. Evidence for such blocks is obtained from the width of X-ray reflections from a metal⁵ which can be interpreted to indicate that the number of dislocation lines is of the order of

$$N_0 \ell = 10^8 \text{ dislocation per sq cm} \quad (3)$$

Here N_0 is the total number of dislocation loops per cubic centimeter and ℓ is the average loop length as shown in the model of Fig. 4. If these dis-

⁴ A. H. Cottrell, loc. cit., p. 62-64.

⁵ A. H. Cottrell, loc. cit., Chapter IV, pp. 99-102.

locations form the edges of a network we must have

$$N_0 \ell^3 \doteq 1 \quad (4)$$

and hence equations (3) and (4) would indicate

$$N_0 \doteq 10^{12}; \quad \ell = 10^{-4} \text{ cm} \quad (5)$$

Data from the etching of crystals⁶ for which pits are delineated at dislocation ends, however, indicate that for aluminum the number of dislocations per square centimeter is in the order of

$$N_0 \ell \doteq 10^5 \text{ to } 10^6 \quad (6)$$

For germanium⁷ the number of dislocations per square cm. is about 10^4 to 10^5 per sq cm.

According to Mott⁸ the most likely form for a network of dislocations is one for which dislocations from three intersecting glide planes meet in a point as shown in Fig. 3. The Burger's vectors then add up to zero and

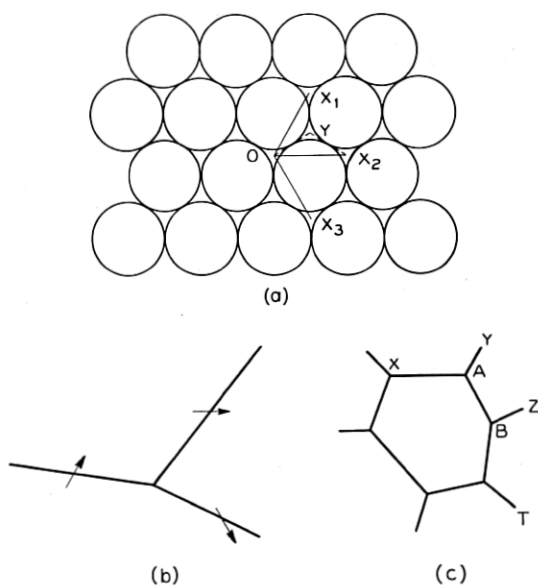


Fig. 3 — Dislocation network forming crystal mosaic (after Mott) (a) A close packed plane, showing the Burgers vector for complete and half dislocations (b) Junction of three dislocations (c) Network of dislocations.

⁶ I. and H. Suzuki, Dislocation Networks in Crystals, Rep. Res. Inst. Tohoku Univ. **A6**, No. 6, Dec., 1954.

⁷ F. Vogel, private communication.

⁸ N. F. Mott, Phil. Mag., **43**, 1151, 1952.

the nodes are stable. A network of such dislocations can outline the mosaic blocks as already discussed. However, the ultrasonic data presented shortly indicate that the effective loops are delineated by impurity atoms rather than by dislocation nodes. This is a possibility even with the model of Fig. 3 if impurity atoms settle along dislocation lines and clamp them at definite points. Impurity atoms having different radii than the solvent atoms are attracted to dislocations since they relieve energy by their presence. If the radius of the impurity atom is smaller than that of the solute atom, the former will take the position shown by the dotted line of Fig. 1 in the compressed region since this position corresponds to lower energy. If the radius is larger than that of the solvent atoms, the impurities will settle in the region of crystal extension.

Using elastic theory Cottrell⁹ has shown that the binding energy of an impurity atom is given by the equation

$$U_B = \frac{4}{3} \left(\frac{1 + \sigma}{1 - \sigma} \right) \frac{\mu b r^3 \epsilon \sin \theta}{R} \quad (7)$$

where r is the radius of solvent atom, $\epsilon = (r' - r)/r$ where r' is the radius of the impurity atom, θ is the angle between the glide plane and the line joining the dislocation center and the impurity atom and R is the distance of the dislocation center from the impurity atom. At low temperatures the dislocation atoms will settle in the position of minimum energy which is $\sin \theta = -1$; $R = r$. Equation (7) was calculated on the basis of elastic theory which is not strictly valid for such large strains. Comparison with experimental values¹⁰ shows that the measured energy is about $\frac{1}{3}$ to $\frac{1}{2}$ that calculated from (7). Hence we take

$$U_B = \frac{1}{3} \left(\frac{1 + \sigma}{1 - \sigma} \right) \mu b^3 \epsilon \quad (8)$$

for a face-centered metal for which $r = b/\sqrt{2}$. Consequently the model considered for a pure single crystal is the one shown in Fig. 4. It consists of the basic network of dislocations shown in Fig. 3 with a distribution of impurity atoms along the dislocations determining the average loop length between pinning points. With this model

$$N_0 \ell^3 \leq 1 \quad (9)$$

The ultrasonic data presented in the next sections indicate that, for aluminum, $N_0 \ell^3 \approx 0.08$, while for lead it is about 0.5.

The fundamental unit considered for ultrasonic attenuation is then the

⁹ A. H. Cottrell, loc. cit., p. 57.

¹⁰ A. H. Cottrell, loc. cit., p. 134.

pinned dislocation of average length ℓ_0 . Such a loop acts like a stretched string and it can be shown¹¹ to have a tension T equal to

$$T = \mu b^2 \quad (10)$$

At absolute zero such loops remain stationary in their minimum energy positions, but as the temperature rises, thermal agitation occurs and a dislocation loop may become displaced to the next minimum energy position. When a dislocation moves from one minimum energy position it has to overcome the shearing stress tending to return it to the mini-

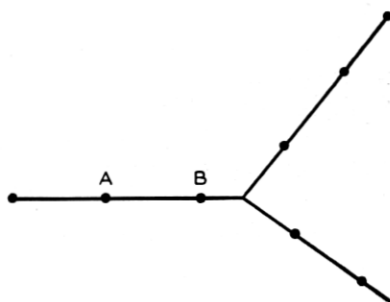


Fig. 4. — Dislocation model with impurity atoms.

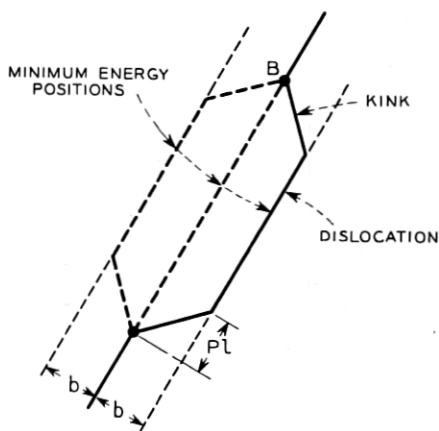


Fig. 5 — Dislocation loop with pinning atoms and form of dislocation loop.

¹¹ A. H. Cottrell, *loc. cit.*, p. 53.

imum energy position; this is usually taken as a sinusoidal stress

$$T_{13} = T_{13_0} b \sin \frac{2\pi x}{b} \quad (11)$$

where T_{13_0} is the limiting Peierls shearing stress required to surmount the barrier and x is the loop displacement. In addition to this, energy is required to stretch the dislocation against its tension T . The model that has usually been considered¹² for this type of motion is the one shown by Fig. 5. This consists of a straight section of dislocation connected to the pinning points by two "kinks" or approximately straight sections of dislocations cutting across between two minimum energy positions. The energy associated with the dislocation loop at any displacement d from a minimum energy position can be calculated as follows. If $p\ell$ is the percentage of the total length of the loop covered by a "kink", the increase in length for a displacement d is

$$\Delta\ell = 2(\sqrt{(p\ell)^2 + d^2} - p\ell) \doteq \frac{d^2}{p\ell} \quad (12)$$

The work done against the tension T is

$$W_1 = T\Delta\ell = \frac{\mu b^2 d^2}{p\ell} \quad (13)$$

Work is also done against the restoring force of (11) in an amount

$$W_2 = T_{13_0} b \int_0^y dy \int_0^{d(y)} \sin \frac{2\pi x}{b} dx \quad (14)$$

Performing the integration, we find that

$$W_2 = \frac{T_{13_0} b^2 \ell}{2\pi} \left[1 - \cos \frac{2\pi d}{b} + 2p \left(\cos \frac{2\pi d}{b} - \frac{b}{2\pi d} \sin \frac{2\pi d}{b} \right) \right] \quad (15)$$

Hence the total energy W is the sum of (13) and (15).

When the loop reaches the next energy minimum, $\cos 2\pi d/b = 1$, and

$$A = \frac{T_{13_0} b^2 p\ell}{\pi} + \frac{\mu b^2 d^2}{p\ell} \quad (16)$$

To obtain the minimum energy, the length $p\ell$ is determined by making W_{\min} a minimum with respect to $p\ell$. Differentiating W_{\min} by $p\ell$ and set-

¹² This type of loop was first considered by N. F. Mott and F. R. N. Nabarro, Dislocation Theory and Transient Creep, Report of a Conference on Strength of Solids, published by The Physical Society, 1948, and has been elaborated by Read, loc. cit., p. 47. Read investigated the conditions for kink stability.

ting the result equal to zero, we find

$$p\ell = \sqrt{\frac{\pi\mu}{T_{130}}} d = \sqrt{\frac{\pi\mu}{T_{130}}} b \quad (17)$$

since $d = b$ at this position. Hence this length is independent of the total loop length. For the ratio of T_{130}/μ found experimentally, i.e., 6.0×10^{-6} , the length of each kink is about

$$p\ell = 720b = 2.5 \times 10^{-5} \text{ cm for lead} \quad (18)$$

The energy for both kinks is from equation (13)

$$W_1 = b^3 \sqrt{\frac{T_{130}\mu}{\pi}} \quad (19)$$

The total energy at the first minimum A is then

$$A = 2b^3 \sqrt{\frac{T_{130}\mu}{\pi}} \quad (20)$$

The energy H , at the maximum, which occurs when $\cos 2\pi d/b = -1$ becomes

$$H = \frac{T_{130}b^2\ell}{\pi} \quad (21)$$

There are other minima at distances $\pm 2b$, $\pm 3b$, etc., on each side of the central position and it can be shown that the successive minima have values of $2A$, $3A$, etc., while the height of the energy barrier remains at H . The question arises as to whether these other positions should be included in the calculation. This model is an ideal situation in which no strains of any kind are permitted in the medium. Actually, impurity atoms above and below the glide plane introduce stresses which distort the dislocation from its straight line position and have the effect of increasing the energies at the bottom of the potential wells. This effect will be much larger for position of $\pm 2b$, $\pm 3b$, etc., and will probably wipe out these minimum energy positions. For the central line and for the positions $\pm b$, the effect is smaller and hence it appears that the model should have only two alternate positions in addition to the central position. For an absolutely pure crystal these other energy positions would probably exist. Calculations including them show that the form of the Q^{-1} curve given by equation (37) is essentially unchanged but that the multiplying constant $\Delta\mu/\mu$ is increased.

The potential well model for a dislocation displaced from its minimum energy position to the next minimum on either side will then be that

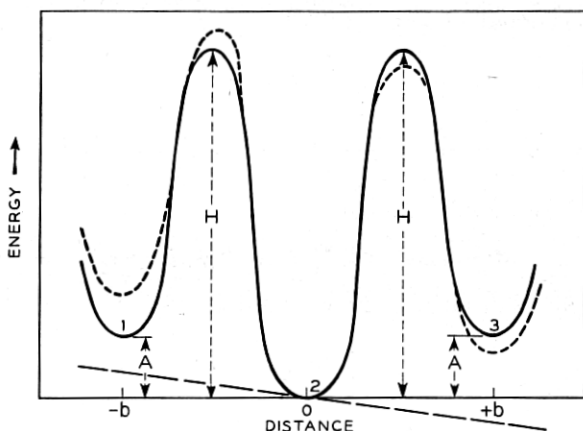


Fig. 6 — Potential well model corresponding to dislocation loop.

shown by Fig. 6. The two energy wells on either side are higher than the center one by the energy A of equation (20). In between these minimum energy positions there are potential barriers of height H given by equation (21). The physical picture given for the process is then that the dislocation vibrates in its lowest potential well (2) until it acquires enough thermal energy to overcome the barrier H and land in wells 1 or 3. According to reaction rate theory, the number of times per second that this process is likely to occur is given by the equation

$$\alpha = \gamma e^{-U/RT} \quad (22)$$

where γ is the number of times that the dislocation attacks the barrier per second, U is the height of the energy barrier and RT the thermal energy. If U is expressed in calories per mole, then R the gas constant per mole is 2 calories per degree increase in temperature. The number of times that the dislocation attacks the barrier should be approximately equal to the resonant frequency of the dislocation in its potential well. Experimentally, it is found that γ is close to $2\pi f = \omega$, the value for the natural vibration.

The resonant frequency of a dislocation in its potential well can be calculated from the restoring force and the mass per unit length which¹³

¹³ J. S. Koehler, Chapter VII, Imperfections in Nearly Perfect Crystals, Wiley, 1952. Koehler considers dissipation to be due to dissipation of freely vibrating dislocations. For the potential well model, freely vibrating dislocations do not exist.

is $\pi\rho b^2$. The restoring force can be determined from the derivative of $(W_1 + W_2)$ with respect to d as d becomes small. The result of differentiation, using equations (13) and (15) is

$$\left[2\pi T_{13_0}\ell + b \sqrt{\pi T_{13_0}\mu} \left(\frac{2}{\pi} - \frac{8}{3} \pi \right) \right] d \quad (23)$$

Since the last term is much smaller than the first, we neglect it, and have the equation

$$\pi\rho b^2\ell \frac{d^2d}{dt^2} + 2\pi T_{13_0}\ell d = 0 \quad (24)$$

For simple harmonic motion $d^2d/dt^2 = -\omega^2d$ so that

$$\pi\rho b^2\ell\omega^2 = 2\pi T_{13_0}\ell \quad (25)$$

Hence the resonant frequency for a dislocation in its potential well is independent of the loop length and equal to

$$f = \frac{1}{2\pi b} \sqrt{\frac{2T_{13_0}}{\rho}} \quad (26)$$

For lead, copper, aluminum, and silver, using the value of $T_{13_0} = 6.0 \times 10^{-6} \mu$, the relaxation values of ω for the metals are

Pb	Cu	Al	Ag	
$\omega = 2\pi f \doteq 7.8 \times 10^9$	2.8×10^{10}	3.6×10^{10}	1.9×10^{10}	(27)

All of these values are considerably higher than any angular frequencies ω which have so far been used. For frequencies approaching these values resonance effects may be expected.

The potential well model of Fig. 6 results in a relaxation type loss and a change in the elastic constant. As with all relaxation effects, energy for low frequency vibrations has time to equilibrate among the various potential wells and is returned at a later part of the cycle without appreciable loss. Since the dislocations can be displaced from their equilibrium positions, a plastic component of strain results and the metal has a greater elastic compliance than would occur without dislocation displacement. As the period of force application becomes comparable with the equilibrating or "relaxation" time an appreciable fraction of the energy is not returned to the vibration but is converted into heat. In this frequency

range, the attenuation becomes a maximum and the elastic constant is intermediate between its high frequency and low frequency values. Finally if the frequency of vibration is sufficiently high there is not time for the dislocation to move from its potential well and the material becomes stiffer and less lossy. At room temperature sufficiently high¹⁴ sonic frequencies have not been used to observe this complete process. However, as one lowers the temperature, the relaxation frequency decreases due to the activation energy term $e^{-U/RT}$ of (22); this process was first observed by Bordoni.¹⁴ An explanation in terms of dislocation loops was first published by the writer.¹⁵

The loss and change in the elastic constant can be obtained by applying reaction rate theory to the model of Fig. 6. The effect of applying a shearing stress along the glide plane is to lower one potential well and raise the other one as shown by the dashed line of Fig. 6. The effect of any other stress is to provide a component of shearing stress in the glide plane and the magnitude of the relaxation effect is then related to the relaxation in the glide plane as discussed in the next section. In general a relaxation measured in one stress system has to be multiplied by a factor F to equal that in the glide plane.

The lowering of the potential well 3 by the shearing stress T_{13} is equal to

$$\Delta = T_{13}b^2\ell(1 - p) \quad (28)$$

Potential well 1 is raised by a similar amount. This results in a redistribution of the number of dislocations in the three types of wells and hence a plastic strain equal to

$$S_{13}^P = (N_3 - N_1)(1 - p)b^2\ell, \quad (29)$$

where $(1 - p)b\ell$ is the area swept out by a single loop. The rate at which the shearing stress changes with time is determined by combining the four transition probabilities for the three wells and since the details of the calculation have been given previously,¹⁶ only the final result is given.

¹⁴ P. C. Bordoni, Elastic and Anelastic Behavior of Some Metals at Very Low Temperatures, *J. Acous. Soc. Am.*, **26**, July, 1954.

¹⁵ W. P. Mason, Dislocation Relaxations at Low Temperatures and the Determination of the Limiting Shearing Stress of a Metal, *Phys. Rev.*, **98**, pp. 1136-1138, May 15, 1955.

¹⁶ W. P. Mason, Relaxations in the Attenuation of Single Crystal Lead at Low Temperatures and Their Relation to Dislocation Theory, *J. Acous. Soc. Am.*, **27**, July, 1955. For other measurements see also paper K4 by B. Welber, Program of the 49th meeting of the Acoustica Society of America, July 2, 1955. The relaxation in lead at 50 kc was shown as a slide. July, 1955.

For finite stresses the formula for the plastic strain takes the form

$$S_{13}^P = \frac{2e^{-A/RT} N_0 (1-p) b^2 \ell \sinh \frac{\Delta}{kT} \cdot \left[1 - \frac{j\omega}{2\gamma} \left(\frac{1 + e^{A/RT}}{\cosh \Delta/2kT} \right) e^{(H-A)/RT} \right]}{1 + 2e^{-A/RT} \cosh \frac{\Delta}{kT} - \frac{j\omega}{\gamma} \cdot (4 + 2e^{-A/RT}) \cosh \frac{\Delta}{2kT} e^{(H-A)/RT} + \frac{3\omega^2}{\gamma^2} e^{2(H-A)/RT}} \quad (30)$$

if H and A are expressed in calories per mole. For stresses such that

$$\frac{\Delta}{kT} = \frac{T_{13} b^2 \ell (1-p)}{kT} \ll 1$$

we can replace the \sinh by the argument and the \cosh by 1. Hence equation (30) reduces to

$$\frac{S_{13}^P}{T_{13}} = \frac{2e^{-A/RT} \left(\frac{N_0 \ell^2 (1-p)^2 b^4}{kT} \right) \cdot \left[1 - \frac{j\omega}{\gamma} \left(\frac{1 + e^{A/RT}}{2} \right) e^{(H-A)/RT} \right]}{\left(1 - \frac{j\omega}{\gamma} \left(\frac{3}{1 + 2e^{-A/RT}} \right) e^{(H-A)/RT} \right) \left(1 - \frac{j\omega}{\gamma} e^{(H-A)/RT} \right)} \quad (31)$$

If we expand the right hand side of (31) into real and imaginary parts, we find

$$\frac{S_{13}^P}{T_{13}} = \frac{2e^{-A/RT} \left[\frac{N_0 \ell^2 (1-p)^2 b^4}{kT} \right]}{1 + 2e^{-A/RT} \left[\frac{N_0 \ell^2 (1-p)^2 b^4}{kT} \right]} \left\{ \frac{1 + \left(\frac{\omega}{\omega_0} \right)^2 \left(\frac{2e^{A/RT} + e^{-A/RT}}{1 + 2e^{-A/RT}} \right) + j \frac{\omega}{\omega_0} \left[\frac{5 + 2e^{-A/RT} - e^{A/RT}}{2(1 + 2e^{-A/RT})} + \left(\frac{\omega}{\omega_0} \right)^2 \left(\frac{3(1 + e^{A/RT})}{2(1 + 2e^{-A/RT})} \right) \right]}{1 + \frac{\omega^2}{\omega_0^2} \left(\frac{10 + 4e^{-A/RT} + 4e^{-2A/RT}}{1 + 4e^{-A/RT} + 4e^{-2A/RT}} \right) + \left(\frac{\omega}{\omega_0} \right)^4 \left(\frac{3}{1 + 2e^{-A/RT}} \right)^2} \right\} \quad (32)$$

and

$$\omega_0 = \gamma e^{-(H-A)/RT}$$

If A is small compared to RT this equation reduces to the usual expression

$$\frac{S_{13}^P}{T_{13}} = \frac{2e^{-A/RT}}{1 + 2e^{-A/RT}} \left[\frac{N_0 \ell^2 (1-p)^2 b^4}{kT} \right] \frac{1 + j \frac{\omega}{\omega_0}}{1 + \left(\frac{\omega}{\omega_0} \right)^2}$$

An intermediate equation is obtained by expanding the three terms of (31) into a series for the two factors in the denominator divided by the factor in the numerator. The first two terms yield in the equation,

$$\frac{S_{13}^P}{T_{13}} = \frac{2e^{-A/RT}}{1 + 2e^{-A/RT}} \left(\frac{N_0 \ell^2 (1-p)^2 b^4}{kT} \right) \left(\frac{1 + j \frac{\omega}{\omega_0}}{1 + \left(\frac{\omega}{\omega_0} \right)^2} \right) \quad (33)$$

$$\text{where } \omega_0 = \frac{\gamma e^{-(H-A)/RT}}{F}$$

and

$$F = \frac{2 + 5e^{A/RT} - e^{2A/RT}}{2(2 + e^{A/RT})}$$

This equation will be used in evaluating the measurements to be discussed in the next section.

If we add to this the purely elastic strains $S_{13}^P = T_{13} \mu^E$, the ratio of the total strain to the applied stress is

$$\frac{S_{13}^P + S_{13}^E}{T_{13}} = \frac{1}{\mu} = \frac{1}{\mu^E} + \frac{2e^{-A/RT}}{1 + 2e^{-A/RT}} \frac{N_0 (1-p)^2 b^4 \ell^2}{kT} \left(\frac{1 + j\omega/\omega_0}{1 + (\omega/\omega_0)^2} \right) \quad (34)$$

This equation shows that the elastic shear modulus μ varies with frequency and the presence of an imaginary term indicates that there is a dissipation associated with this relaxation. For the real part we find

$$\frac{\mu^E - \mu}{\mu} = \frac{\Delta\mu}{\mu} = \left(\frac{2e^{-A/RT}}{1 + 2e^{-A/RT}} \right) \frac{N_0 \ell^2 (1-p)^2 b^4}{kT} \mu^E \left(\frac{1}{1 + \omega^2/\omega_0^2} \right) \quad (35)$$

The total change in elastic constant $\Delta\mu^0$ which occurs when the frequency goes from zero to infinity is then

$$\frac{\Delta\mu^0}{\mu^0} = \left(\frac{2e^{-A/RT}}{1 + 2e^{-A/RT}} \right) \frac{N_0 \ell^2 (1-p)^2 b^4 \mu^E}{kT} \quad (36)$$

Since the imaginary part of (34) represents the dissipation of energy it

can be shown that

$$\frac{1}{Q} = \frac{\Delta\mu^0}{\mu^0} \frac{\omega/\omega_0}{1 + (\omega/\omega_0)^2}. \quad (37)$$

These are the equations connected with a single relaxation which, in this case, would be associated with the displacement of a single length dislocation. Since there is a distribution of loop lengths about the most probable value, the activation energy, H , will vary and hence each length will have a different relaxation frequency. Equations (35) and (37) can be generalized to the forms

$$Q^{-1} = \sum_{i=1}^n \frac{\Delta\mu_i}{\mu_0} \left(\frac{\omega/\omega_i}{1 + (\omega/\omega_i)^2} \right); \quad \frac{\mu}{\mu_0} = 1 + \sum_{i=1}^n \frac{\Delta\mu_i}{\mu_0} \left(\frac{(\omega/\omega_i)^2}{1 + (\omega/\omega_i)^2} \right) \quad (38)$$

As will be discussed in the next section, these equations can be used to evaluate the characteristics of a relaxation at low temperatures which is connected with the displacement of dislocations from their minimum energy positions to adjacent minimum energy positions. In the process they give experimental evidence on the limiting shearing stress in metals, on the number of dislocations per square centimeter in metals and on the average loop lengths. The values found are in good agreement with other methods for measuring these properties.

EXPERIMENTAL EVIDENCE FOR DISLOCATION RELAXATIONS AT LOW TEMPERATURES

The first experimental evidence for a relaxation at low temperatures was provided by the work of Bordoni.¹⁴ Using an electrostatic drive method, Bordoni measured the inverse Q values for a number of metals down to liquid helium temperatures. All these measurements were made with very small strains, i.e., less than 10^{-8} , which are in themselves too small to displace dislocations from their minimum energy positions. They can, however, bias the potential wells of the model of Fig. 6. Then, temperature induced motions arise so that, for slowly applied motions, equilibrium of dislocation distributions can occur between the potential wells, with the applied stress thereby superimposing a plastic strain on the elastic strain. For very high frequencies there is not time for the dislocations to redistribute themselves and only the elastic strain occurs. This process results in a relaxation which extends over a frequency range. As discussed in the previous section, the dislocations have too high a natural frequency for this process to be observed at room temperature.

All of Bordoni's measurements were made for polycrystals or single crystals of a definite length, i.e., 6.4 cms. The natural resonance fre-

angular relaxation frequencies $\omega_0 = 2\pi f_0$ can be represented by the equation

$$\omega_0 = 5.3 \times 10^9 e^{-975/RT} \quad (40)$$

so that we are dealing with a process having an activation energy of about 975 calories per mole. This is a very low activation energy and the only known process which has as low an energy as this is the one discussed in the previous section, namely, the displacement of a dislocation, by one atomic spacing, against the limiting shearing stress of the crystal.

To show that this is of the right order of magnitude, we may evaluate the activation energy of the process from (20) and (21):

$$H - A = \left[\frac{T_{130} b^2 \ell}{\pi} - 2b^3 \sqrt{\frac{T_{130} \mu}{\pi}} \right] \frac{6.025 \times 10^{23}}{4.182 \times 10^7} \text{ (cal./mole)} \quad (41)$$

As will be shown presently, the energy average loop length is of the order of 4×10^{-4} cm and since it is known that

$$b = 3.5 \times 10^{-8} \text{ cm}; \quad \text{and} \quad \mu = 7.0 \times 10^{10} \text{ dynes/cm}^2 \quad (42)$$

we find for the limiting shearing stress a value of 4.8×10^5 dynes/cm².

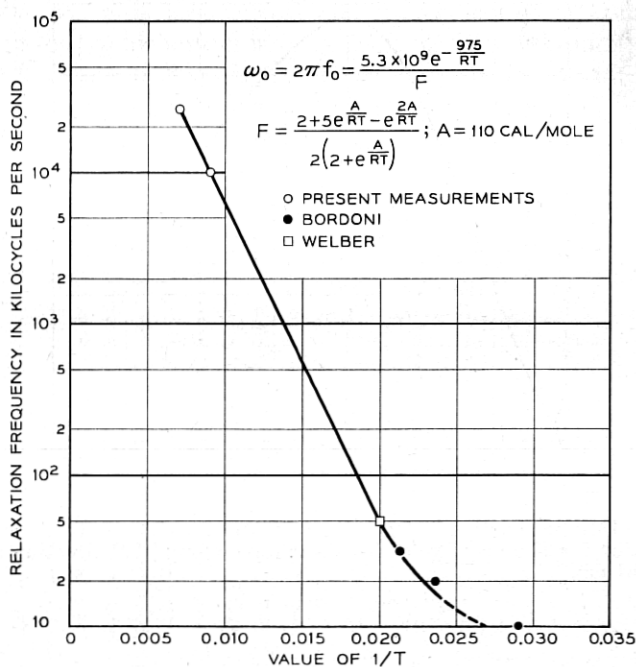


Fig. 9 — Plot of log of relaxation frequency against $1/T$.

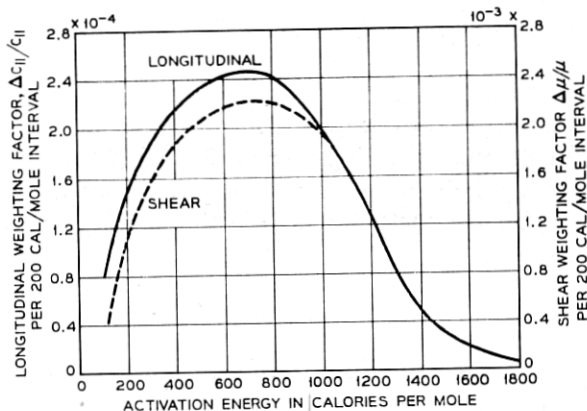


Fig. 10 — Weighting factors for longitudinal and shear waves plotted against activation energies.

Due to the factor, F , a slightly nonlinear relation is obtained between the relaxation frequencies and the reciprocal of the temperature as shown in Fig. 9. Hence we find

$$T_{13_0} = 4.8 \times 10^5 \text{ dynes}; \quad T_{13_0}/\mu = 6.8 \times 10^{-6} \quad (43)$$

values in good agreement with Peierls' lower theoretical value in (1). The value of $\gamma = 5.3 \times 10^9$ is within a factor of 1.5 of the calculated angular resonance frequency of a dislocation in its potential well as given by (26).

In calculating T_{13_0} an assumed value was used for the average length of a dislocation loop. Some evidence on the size of the dislocation loops and their distribution around the average size can be obtained from the data of Fig. 8 for the attenuation measured in a lead single crystal. The form of the $1/Q$ curve for a single loop length is given by (32). The best fit to the measured values is shown by the dashed curve of Fig. 8(a), and, as can be seen therein, a single relaxation does not agree fully with the measured values. If we assume a distribution of activation energies, the measured curves can be fitted by using the weighting function given in Fig. 10. This verifies the existence of loops shorter and longer than the mean value, in agreement with the model shown in Fig. 4. Since the measured activation energies, $H - A$, are nearly proportional to the loop lengths, the distribution in activation energies also corresponds to the distribution of loop lengths. The distribution function for the shear measurements is also shown in Fig. 10. The height of the shear curve is about 9 times as high as that for the longitudinal measurement. It will be

evident from subsequent discussion of equation (45) that this is to be expected. The number of dislocations for the shear crystal is about 40 per cent higher than for the longitudinal crystal.

Some data on the average loop length can be obtained from the data of Fig. 8(a). If we consider a single loop length as shown by the dashed curve and increase the maximum until the area under the loop is equal to that under the measured curve, the value of the weighting factor $\Delta c_{11}/c_{11}$ becomes

$$\frac{\Delta c_{11}}{c_{11}} = 8.4 \times 10^{-4} \quad (44)$$

Since all the formulas used in dislocation theory refer to isotropic materials rather than cubic crystals, we take

$$c_{11} = \lambda + 2\mu$$

To determine how a measured change in $\Delta c_{11}/c_{11}$, determines a weighting factor $\Delta\mu/\mu$, we note that the bulk modulus, B , does not have any relaxation effect, i.e., a pure compression will cause no shearing motion in the glide plane. Since

$$B = \lambda + \frac{2}{3}\mu; \quad \Delta B = \Delta\lambda + \frac{2}{3}\Delta\mu = 0; \quad \text{Hence} \quad \Delta\lambda = -\frac{2}{3}\Delta\mu$$

Therefore

$$\frac{\Delta c_{11}}{c_{11}} = \frac{\Delta\lambda + 2\Delta\mu}{\lambda + 2\mu} = \left(\frac{\frac{4}{3}\Delta\mu}{\mu}\right) \frac{\mu}{\lambda + 2\mu}, \quad (45)$$

and $\frac{\Delta\mu}{\mu} = \frac{3}{4} \left(\frac{\lambda + 2\mu}{\mu}\right) \frac{\Delta c_{11}}{c_{11}}$

It is readily shown that the relation between the change in Young's modulus and the shearing modulus is

$$\frac{\Delta\mu}{\mu} = \frac{3\mu}{Y_0} \left(\frac{\Delta Y_0}{Y_0}\right), \quad (46)$$

a relation needed later.

From (35), (44), and (45), we have

$$4.3 \times 10^{-3} = \frac{2e^{-AR/T_0}}{1 + 2e^{-A/RT_0}} \left[\frac{\bar{N}\ell(1-p)^2 b^4}{kT_0} \right] \mu^E \quad (47)$$

where $\bar{N} = N_0\ell$ is the number of dislocations per square centimeter, which is a measurable quantity if one uses the etch technique.

Since $A = 110$ calories per mole, $T_0 = 140^\circ\text{K}$, $(1-p)^2 = 0.90$; $b = 3.5$

$\times 10^{-8}$; $k = 1.38 \times 10^{-16}$ and $\mu^E = 7.0 \times 10^{10}$ dynes per sq cm we find

$$\bar{N}\ell \doteq 1.3 \times 10^3 \quad (48)$$

Data from the mechanical hysteresis effect discussed in the next section indicate that

$$\bar{N} \doteq 3.1 \times 10^6 \quad (49)$$

and hence the average loop length is about

$$\ell \doteq 4 \times 10^{-4} \text{ cm} \quad (50)$$

Hence we have

$$\bar{\ell} \doteq 4 \times 10^{-4} \text{ cm}, \quad \text{and} \quad N_0 \bar{\ell}^3 \doteq 0.5 \quad (51)$$

One can use the measurements of Bordoni shown in Fig. 7 to show that the present interpretation, attributing the relaxation to the displacement of a dislocation by one atomic spacing against the limiting shear stress of the crystal, is consistent for several face-centered metals. Since the temperature of maximum attenuation results when the measuring frequency equals the relaxation frequency we have

$$\frac{\omega}{\gamma e^{-(H-A)/RT}} = 1$$

Since the ratio of each measuring frequencies listed in (39) to the corresponding resonant frequency for dislocations (27) is nearly a constant, the activation energy, $H - A$, will be proportional to the temperature of maximum loss. The activation energy of lead was evaluated as 975 calories per mole at a temperature of 35°K. Hence, we can evaluate the activation energy of each metal; as shown in Table II, the average value of (T_{130}/μ) is about 6×10^{-6} .

In view of the approximate nature of this calculation (including the tacit assumption that all the loop lengths are the same for the different metals), the results in Table II constitute satisfactory confirmation of the

TABLE II

Metal	Temp. of Max. Atten.	H-A in cal/mole	b in $\text{cm} \times 10^8$	μ dynes/cm ²	T_{130} dynes/cm ²	T_{130}/μ
Pb	35°K	975	3.5	7.0×10^{10}	4.8×10^5	6.8×10^{-6}
Cu	85°K	2360	2.55	4.6×10^{11}	2.4×10^6	5.2×10^{-6}
Al	100°K	2760	2.86	2.5×10^{11}	1.9×10^6	7.6×10^{-6}
Ag	60°K	1710	2.88	2.7×10^{11}	1.3×10^6	4.8×10^{-6}

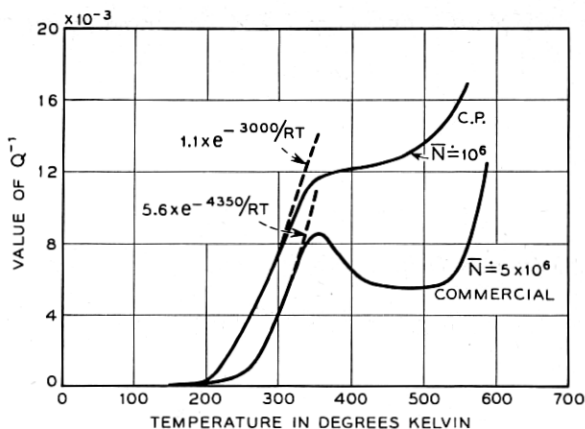


Fig. 11 — Higher temperature values of mechanical hysteresis effect (Bordoni and Nuovo).

proposed origin of the relaxation frequency. The values found are in good agreement with the most probable values given by Cottrell.⁴

TEMPERATURE ACTIVATED MECHANICAL HYSTERESIS MECHANISMS

In addition to the relaxation mechanism discussed in the last section, the measured values in Figs. 8 show that there is another source of loss which is independent of frequency for a given specimen. Fig. 11 shows an extension of the measurements of Bordoni, by Bordoni and Nuovo,¹⁷ to a higher temperature for pure and commercial lead. Both materials show an increase in attenuation of the form

$$Q^{-1} = Ce^{-U/RT}$$

with the values

pure lead

$$C = 1.1; \quad U = 3000 \text{ cal/mole}; \quad \text{and} \quad (52)$$

commercial lead

$$C = 5.6; \quad U = 4350 \text{ cal/mole.}$$

Above 350°K, this increase reaches a maximum and then drops off. A similar rise was found by Ké¹⁸ for aluminum single crystals at 0.8 cycles

¹⁷ P. G. Bordoni and M. Nuovo, Sulla Dissipazione Delle Onde Elastiche Nel Piombo Ad Alta Temperatura, *Il Nuovo Cimento*, **11**, pp. 127-140, Feb. 1, 1954.

¹⁸ T. S. Ké, Experimental Evidence of the Viscous Behavior of Grain Boundaries in Metals, *Phys. Rev.*, **71**, p. 533, 1947. See also C. Zener, *Elasticity and Anelasticity of Metals*, p. 151, Fig. 48, Chicago Univ. Press, 1948.

as shown in Fig. 12. This rise follows the same formula with

$$C = 0.37 \quad \text{and} \quad U = 5200 \text{ cal/mole} \quad (53)$$

Since this effect is independent of frequency it is called a temperature activated mechanical hysteresis.

The model of Fig. 4 admits only two possibilities. One is that the pinning points can momentarily be torn from the dislocation, thereby allowing energy to be transmitted from one loop to the other. The other possibility is that thermal energy will be sufficient to generate an unstable Frank-Read loop which will carry off energy. It is readily shown, however, that it would require 10,000 times the activation energy to cause the loop breakdown and hence the Frank-Read loop cannot be the mechanism. As discussed later, the energy required to remove an impurity atom is of the right order of magnitude and hence this is considered the cause of the hysteresis loss.

The question is how a momentary breakaway of a pinning point can abstract energy from the vibration. All the loops undergo thermal vibration with a velocity determined by the equation

$$\frac{1}{2}(\dot{x}_T)^2 m = kT \quad (54)$$

where m is the mass of the loop which is $\pi\rho b^2\ell$, where ρ is the density of the medium, and \dot{x}_T is the thermal velocity as the loop crosses the equilibrium position. For lead, with loops of 4×10^{-4} cm in length, the mass of the dislocation is about 1.7×10^{-17} grams so that the thermal vibration velocity is about 70 cm/sec at room temperature. This is large

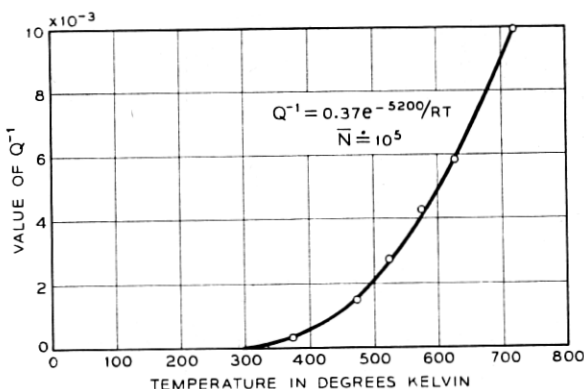


Fig. 12 — Temperature activated mechanical hysteresis effect in aluminum single crystal (after Ké).

compared to the velocity of any particle in the crystal. However, the particle velocity \dot{u} can add to or subtract from the thermal motion when \dot{u} and \dot{x}_T are in or 180° out of phase; hence the energy of vibration may be written

$$\frac{1}{2}(\dot{x}_T + \dot{u})^2 m + \frac{1}{2}(\dot{x}_T - \dot{u})^2 m = (\dot{x}_T + \dot{u})^2 m$$

since it is equally probable for the thermal velocity to add or to subtract from the particle velocity. As long as the loop is pinned at the ends, this energy is returned to the crystal vibration without loss since the vibrations are coherent. When a pinning point is broken, on the average, energy equal to

$$\frac{(\dot{u})^2 m}{2} \quad (55)$$

is abstracted from each loop and since two loops are involved for each impurity atom, an energy of $\dot{u}^2 m$ is abstracted from the crystal vibration.

To calculate the acoustic loss to be expected from this source, consider a shear strain of the form shown in Fig. 13 to be propagated in the direction perpendicular to the glide plane. At $t = 0$, the particle displacement is zero at $x = 0$ and u at $x = \ell$. After an interval of time dt , the strain will be displaced a distance $V_s dt$, where V_s is the shear velocity which is 8.0×10^4 cm/sec for lead. The particle velocity \dot{u} is a constant over the time of the wave. The energy lost in going a distance $\ell_t = V_s dt$ can be calculated as follows. The energy lost per dislocation vibration is $m(\dot{u})^2/2$. For an interval of time dt this has to be multiplied by $f dt$ where f is the frequency of vibration of a dislocation. Hence the loss from a

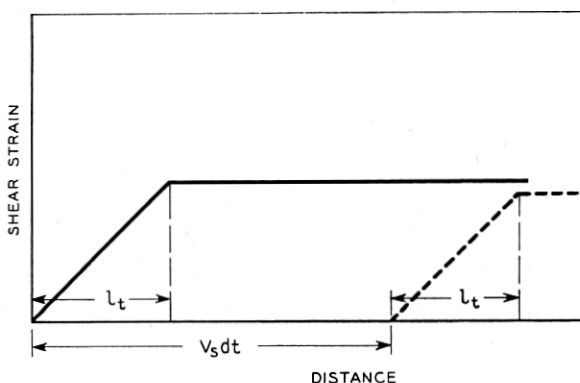


Fig. 13 — Form of shear wave for calculating mechanical hysteresis losses.

single unpinned vibration, in time dt is

$$\dot{u}^2 m f dt = \frac{\dot{u}^2 (\pi \rho b^2 \ell) \sqrt{\frac{2T_{130}}{\rho}}}{4\pi b} = \frac{\dot{u}^2 b \ell \sqrt{\frac{T_{130} \rho}{2}}}{2} dt \quad (56)$$

To get the total loss we have to multiply this by the number of unpinned dislocation loops. From Boltzmann's principle, the number of unpinned loops per cc will be

$$2N_0 e^{-U/RT} \quad (57)$$

where N_0 is the number pinned loops per cc and U the activation energy for tearing an impurity atom away. We have to multiply this by the volume of the disturbance which may be written $V_s dt$ if a unit cross-sectional area is considered. Hence the total loss in time dt is

$$\left(\dot{u}^2 \sqrt{\mu \rho} \sqrt{\frac{T_{130}}{2\mu}} V_s N_0 e^{-U/RT} \right) (dt)^2 \quad (58)$$

The total input energy for the wave, in time dt , is

$$W_0 = \dot{u}^2 \sqrt{\mu \rho} dt, \quad (59)$$

where $\sqrt{\mu \rho}$ is the characteristic impedance of the medium. Hence the energy transmitted in the first interval of time dt takes the form

$$W = W_0 \left[1 - \frac{\left(\sqrt{\frac{2T_{130}}{\mu}} b V_s N_0 e^{-U/RT} \right) dt}{2} \right]. \quad (60)$$

This is the first term of the expansion of the equation

$$W = W_0 e^{-\frac{\left(\sqrt{\frac{2T_{130}}{\mu}} b V_s N_0 e^{-U/RT} \right) dt}{2}} = W_0 e^{-\delta t}$$

where δ is the decrement. Since the decrement $\delta = \pi/Q$, we have finally

$$\frac{1}{Q} = \frac{\sqrt{\frac{2T_{130}}{\mu}} b V_s N_0 e^{-U/RT}}{2\pi} \quad (62)$$

This loss is independent of frequency since it does not depend on ℓ , which determines the steepness of the displacement-time curve. It does not depend on the amplitude up to a strain which can cause breakaways due to the applied strain alone.

To see if (62) yields a reasonable value for a single crystal, assume a temperature of 250°K for which measurements in Fig. 8 along the [100]

direction show that $Q^{-1} = 1.55 \times 10^{-4}$. Multiplying this by 5.2, [see equation (45)], to give the value for a shear wave propagated along the [111] direction we have

$$\frac{1}{Q} = 8.0 \times 10^{-4} \quad (63)$$

$$= \frac{3.48 \times 10^{-3} \times 3.5 \times 10^{-8} \times 8.0 \times 10^4 \times 1.7 \times 10^{-4} (N_0 \ell)}{2\pi}$$

Solving for $N_0 \ell$, the number of dislocations per sq cm, we have

$$\bar{N} = N_0 \ell \doteq 3.1 \times 10^6 \quad (64)$$

If we perform the same calculations with the data for polycrystalline lead, multiplying the resultant values of Q^{-1} by

$$\frac{\Delta\mu}{\mu} = \frac{3\mu}{Y_0} \left(\frac{\Delta Y_0}{Y_0} \right) = 1.2 \frac{\Delta Y_0}{Y_0}, \quad (65)$$

we find

C. P. lead	Commercial lead	
$\bar{N} = 1.2 \times 10^6$	$\bar{N} \doteq 6 \times 10^6$	(66)

Hence the number of dislocations for an unstrained single crystal or polycrystal appears to be in the neighborhood of 10^6 to 6×10^6 .

A somewhat lower value is found for aluminum from the data of Fig. 12. This curve shows an increase in Q^{-1} for a single crystal which can be represented by the equation

$$Q^{-1} = 0.37e^{-5200/RT} \quad (67)$$

These measurements were made for a single crystal wire using a torsional oscillation of 0.8 cycles per second. Since this is for a shear vibration, no correction will be required in the isotropic approximation. To make this agree with equation (62) for $b = 2.86 \times 10^{-8}$ and $V_s = 3 \times 10^5$ cm/sec, we must have

$$\bar{N} = N_0 \ell = 10^5 \quad (68)$$

which is in fair agreement with the values of 10^5 to 10^6 determined from etch pit data.

This temperature actuated mechanical hysteresis is a property of all the metals measured at high temperatures as is shown by the data of Ké¹⁹ given in Fig. 14(a). Here a peak associated with grain boundary

¹⁹ J. S. Ké, J. Appl. Phys., **21**, p. 414, 1950.

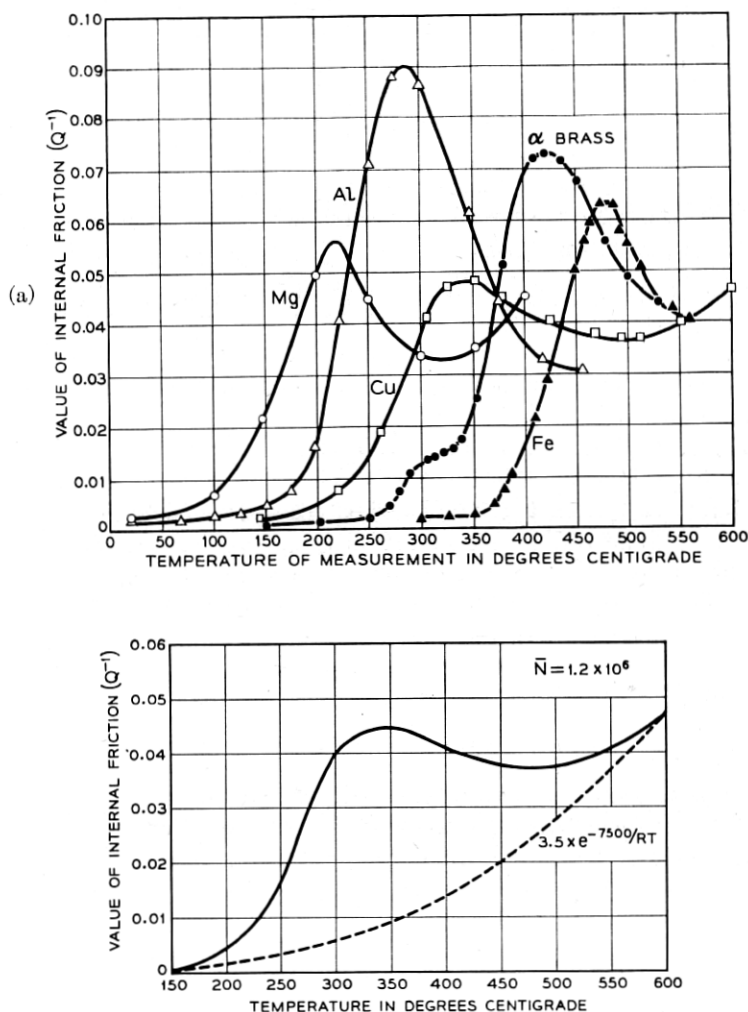


Fig. 14 — (a) Mechanical hysteresis and grain boundary losses in several polycrystalline metals, (b) Separation of losses for copper (after Ké).

motion (discussed in the next section) is followed by an exponentially rising value of internal dissipation as measured by Q^{-1} . The curve for copper is shown in detail in Fig. 14(b). We can separate out the grain boundary loss from the hysteresis loss as shown by the dashed line. This curve can be represented by the equation of the figure with a constant $C = 3.5$ and an activation energy of 7500 calories per mole. Analysis

similar to that outlined for lead and aluminum yields about 1.2×10^6 for the number of dislocations per sq cm.

It remains to be shown that the theoretical activation energy for unpinning a pinning point is of the right order of magnitude to agree with experiment. The binding energy of an impurity atom is given by (8). To obtain $U = 3,000$ to $4,350$ calories per mole for lead, $5,200$ for aluminum, and $7,500$ for copper, we must have the following ratios of impurity atom radius to metal atom radius;

$$\text{Pb}; \quad \epsilon = 0.108 \text{ to } 0.156; \quad \text{Al}; \quad \epsilon = 0.102; \quad \text{Cu}; \quad \epsilon = 0.11 \quad (69)$$

These values are close to what would be expected for the principal impurities which are bismuth and antimony for lead, iron and copper for aluminum, and silicon for copper.

This process should be present for all metals but the activation energy is usually too high for this effect to be observed at room temperature. For lead, as seen from Fig. 11, the effect reaches a maximum at a temperature of about 350°K . This temperature is not far from the critical temperature T_0 of a Cottrell atmosphere, for which the impurity atoms cease to be condensed around a dislocation but, due to thermal agitation, form a "Maxwell" atmosphere around the dislocation. The energy to pull the dislocation away from the atmosphere increases and the number of free dislocation loops decreases. This temperature²⁰ is

$$T_0 = U/R \log (1/c_0) \quad (70)$$

where c_0 is the concentration of impurities in the metal.

For room temperature measurements for most single crystals and unstrained polycrystals, it appears that most of the loss is due to the relaxation mechanism previously discussed. This loss becomes nonlinear with amplitude for large amplitudes as shown by the measurements of Nowick²¹ for copper single crystals. These results are shown in Fig. 15. For strain amplitudes above 1×10^{-7} , the value of Q^{-1} increases as a function of increasing amplitude. Similar results have been found by Read²¹ and others. This can be expected from the model of Fig. 6. When the value of

$$\frac{\Delta}{kT} = \frac{T_{13}b^2\ell(1-p)}{kT} = 1, \quad (71)$$

the argument can no longer replace the sinh. For copper, this corresponds

²⁰ A. H. Cottrell, *Dislocations and Plastic Flow in Crystals*, p. 141. Oxford University Press, 1953.

²¹ A. S. Nowick, *Phys. Rev.*, **80**, p. 249, 1950. T. A. Read, *Trans. A.I.M.E.*, **143**, p. 30, 1941.

to

$$T_{13} = \frac{1.38 \times 10^{-16} \times 300}{(2.55 \times 10^{-8})^2 \times 4 \times 10^{-4}} = 1.6 \times 10^5 \text{ dynes/cm}^2 \quad (72)$$

Since the shear modulus is 4.6×10^{11} dynes cm^2 , this corresponds to a strain of 3.5×10^{-7} . Furthermore, the potential well model is no longer adequate since the dislocations can be displaced by several atomic spacings and their ultimate displacement will be determined by the increase in length of the dislocation. Hence the nonlinear effect is consistent with consideration of the dislocation loop displacement as the cause of dissipation in a metal crystal.

It has been found that the larger the number of impurities, and hence the shorter the loop length ℓ , the larger is the stress required to make Q^{-1} vary non-linearly. This is in agreement with (71). Also since the attenuation is proportional to the number of dislocations \bar{N} times the average loop length ℓ the effect of increased impurities is to lower ℓ and also the attenuation. On the other hand the hysteresis loss depends directly on the number of dislocations only, and should be independent of the impurity content. This appears to be borne out by the data for the pure single crystal, 99.99 pure, in Fig. 8 and for the commercial ma-

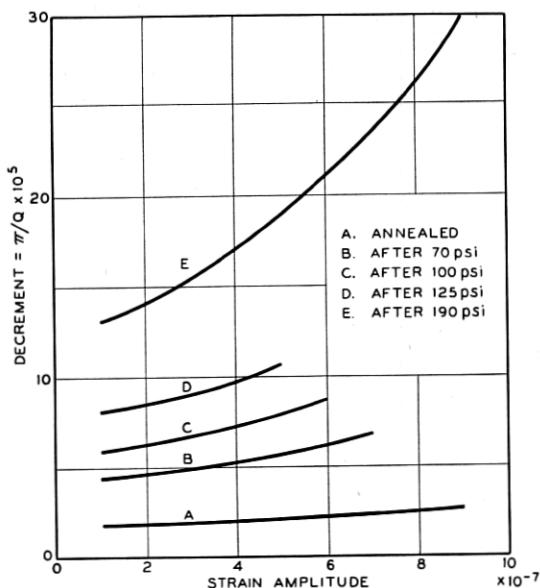


Fig. 15 — Internal friction in copper at room temperature as a function of cold work and strain amplitude (after Nowick).

terial in Fig. 11. An extension of the measurements of Fig. 8 to higher temperatures shows that the hysteresis attenuation reaches its maximum at 260°K and decreases for higher temperatures. This lowering of the peak from 350°K to 260°K, by the increased purity of the lead, is consistent with (70) for the Cottrell atmosphere temperature. Below the peak, however, when one multiplies the crystal value $C = 0.92$ by 5.2 and the polycrystal value C by 1.2, to reduce them to the values for the glide plane, the two values are within a few per cent of each other. Hence the effect of impurities appears to be small for the hysteresis term.

VISCOUS GRAIN BOUNDARY LOSSES

For polycrystals, another dislocation relaxation effect occurring in grain boundaries, contributes to acoustic loss at high temperatures and low frequencies. The boundaries²² between grains of different orientations are regions of vacancies and considerable strain in the lattice. One of the simplest types of grain boundaries, called the Burgers boundary, is shown by Fig. 16. Here two slightly misoriented crystals are made to join by a

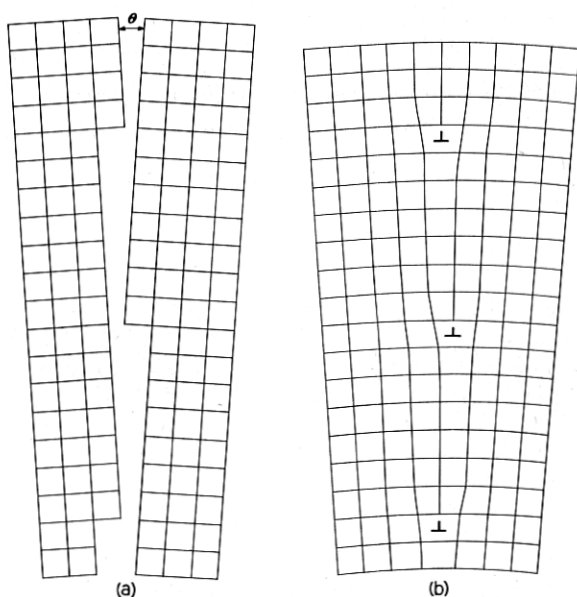


Fig. 16—Burgers dislocation grain boundary with dislocations along cube edges (after Read).

²² A complete discussion of dislocation grain boundary models is given by W. T. Read, *Dislocations in Crystals*, Chapters 11 to 14, McGraw-Hill Co.

series of edge dislocations whose spacings depend on the angle of misfit. Such a grain boundary can be made to glide on the application of a shearing stress, as has been shown by Parker and Washburn.²³ More complex boundaries occur when the plane of joining is not a cube edge. For such boundaries as shown in Fig. 17, two sets of dislocations are required to join the two differently oriented crystals. This type of boundary is called a tilt boundary. If the two grains are given a relative rota-

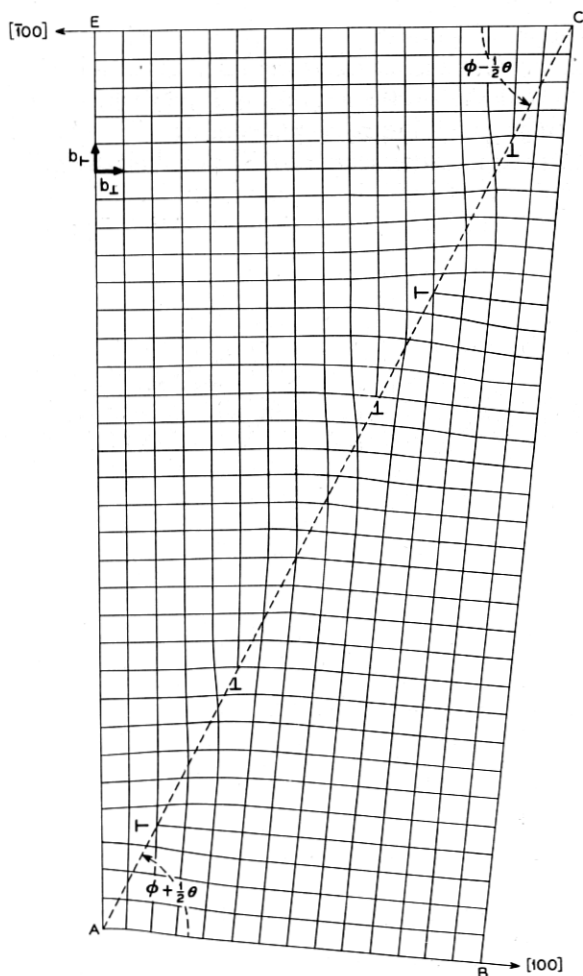


Fig. 17 — Read-Shockley dislocation tilt boundary with two sets of dislocations.

²³ Trans. A.I.M.E., 194, pp. 1076-1078, 1952.

tion with respect to each other, the dislocations connecting them are of the screw type and such boundaries are called twist boundaries.

In the more complicated types of boundaries, the motion cannot be simple glide as in the boundary of Fig. 16 because, due to the various dislocation systems, glide requires sending one set of dislocations through the other and such a motion is strongly resisted. Such a boundary can move only if atoms diffuse into adjacent vacancies and this takes place only at high temperatures where thermal energies can overcome the high activation energies of diffusion. Hence when a cyclic stress is applied to a polycrystal, there is not enough time for a grain boundary to move appreciably so that the elastic constant of a polycrystal does not differ much from a single crystal at room temperature.

Fig. 18 shows the measurements of $K\epsilon^{24}$ on the elastic and dissipation properties of polycrystals and single crystals of aluminum for a torsional vibration at 0.8 cycles, between 100°C and 450°C. The measurements

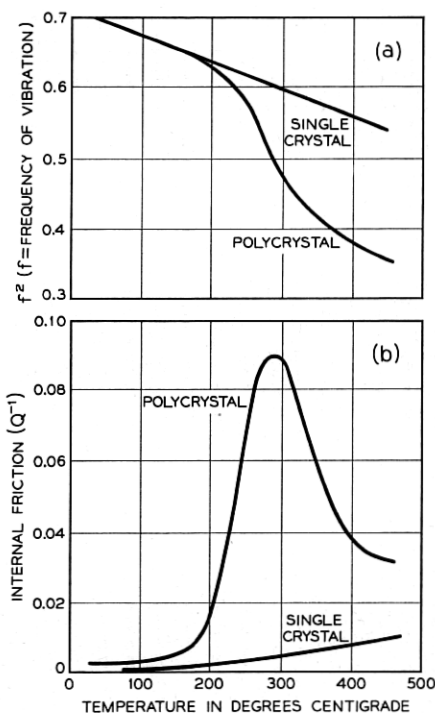


Fig. 18 — Elastic constants and internal dissipation in polycrystal and single crystal aluminum showing grain boundary effect (after Ké).

²⁴ T. S. Ké, Phys. Rev., **70**, p. 105A, 1946, and **71**, p. 533, 1947.

show a relaxation for the polycrystal but none for the single crystal. Both crystal types, however, show the hysteresis effect. By measuring the temperature shift of the maximum attenuation as the driving frequency is changed, Ké found an average activation energy of about 31,000 calories per mole, which is approximately 3.5 kilocalories under the self-diffusion constant of about 34.5 kilocalories per mole for aluminum in aluminum. This decrease of the average value is probably due to the average shearing stress exerted along the boundary. Shearing stress can lower the activation energy for diffusion, as has been shown by the measurement of diffusion bonding in solderless wrapped connections.²⁵ The measurements of Ké confirm the fact that grain boundaries can only move by diffusion of their components under a stress bias. With an activation energy of 31,000 calories per mole, the equation for the angular relaxation frequency becomes

$$\omega_0 = 4 \times 10^{12} e^{-31,000/RT} \quad (73)$$

The value of 4×10^{12} is close to what one would expect for the vibration of a molecule in its own potential well and agrees with the idea that the fundamental process is the motion of the domain wall by diffusion of its separate parts.

The breadth of the relaxation is greater than would be expected for a single activation energy. In fact it requires an activation energy distribution from 27.5 kilocalories to 34.5 kilocalories to account for the width. If we compare this with the measured²⁵ activation energy curve as a function of shear stress, shown in Fig. 19, this range can be explained by shear stresses ranging from 0 to 2000 pounds per square inch with an

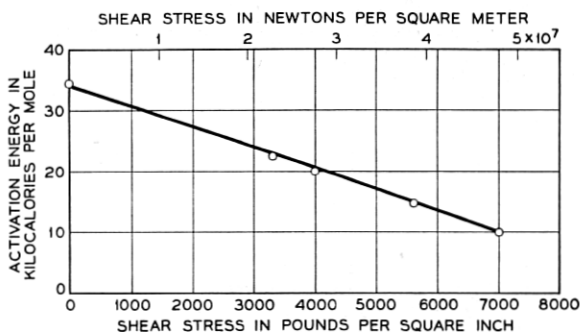


Fig. 19 — Lowering of activation energy of diffusion in aluminum by the application of a shearing stress.

²⁵ W. P. Mason and O. L. Anderson, Stress Systems in the Solderless Wrapped Connection and Their Permanence, B.S.T.J., **33**, pp. 1093-1111, Sept., 1954.

average value of 1,000 pounds per square inch. The strength of the relaxation shows that when the motion of the domain walls can adjust in a time much less than one period, about $\frac{1}{3}$ of the strain occurs by grain boundary motion and $\frac{2}{3}$ by elastic straining.

EFFECTS OF SMALL AND LARGE AMOUNTS OF COLD WORK ON ACOUSTIC ATTENUATION IN METALS

The curves of Bordoni, shown by Fig. 7 and Nowick in Fig. 15 show that small amounts of cold work can increase the attenuation due to the relaxation effect previously discussed. Since the activation energy does not change, the indications are that this increase is due to the production of more dislocations lying along minimum energy positions. An increase in dislocations by factors of 10 or more can occur by this process.

When large amounts of cold work are applied to metals, two other effects have been discovered by Köster²⁶ and his collaborators. The first effect, as shown in Fig. 20, consists of a temporary decrease of the

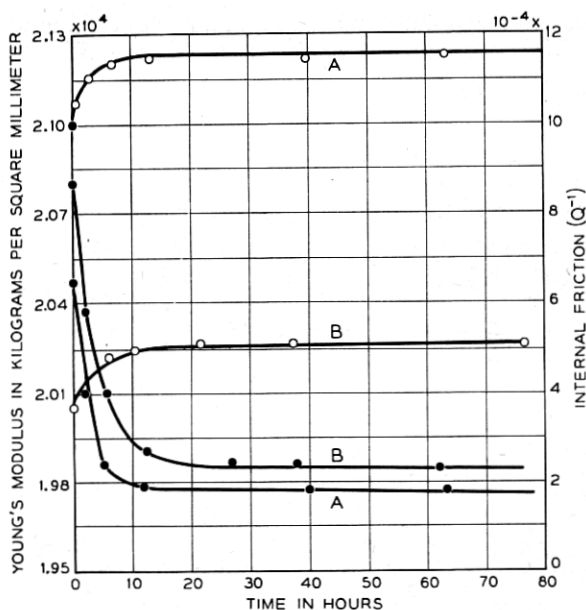


Fig. 20 — Internal friction (solid circles) and dynamic Young's modulus (open circles) of Armco iron, measured at 20°C as a function of time after deformation. Degree of cold drawing: A — 25 per cent, B — 80 per cent. (After Köster.)

²⁶ W. Köster and K. Rosenthal, *Z. Metallkunde*, **30**, p. 345, 1938; W. Köster, *Arch. Eisenhüttenw.*, **14**, p. 271, 1940-41; and F. Förster and W. Köster, *Naturwiss.*, **25**, p. 436, 1937.

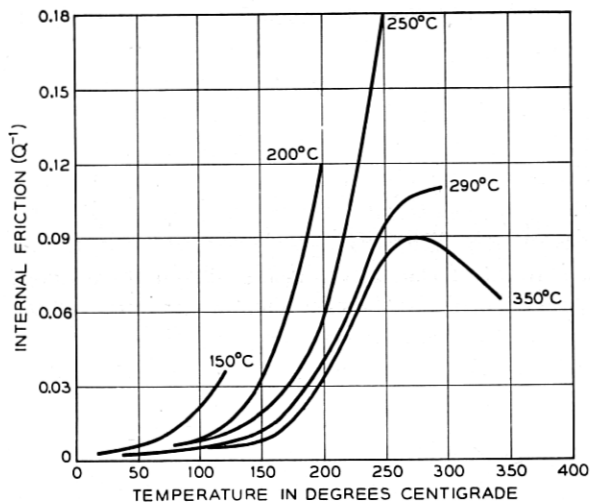


Fig. 21 — Dependence of internal friction of heavily cold worked aluminum on the temperature of measurement, after a series of anneals. The corresponding annealing temperature is marked at the top of each curve (after Ké).

Young's modulus and an increase in the internal friction which relax out in several hours at room temperature, i.e., far below a recrystallization temperature. For very high values of cold drawing, i.e., 80 per cent, a permanent change occurs in the value of Young's modulus until the metal is recrystallized. Although complete measurements²⁷ have not been made it appears that this effect is independent of amplitude for strains up to 10^{-5} , and is not strongly dependent on frequency or temperature from -100°C to 0°C . This effect has been called the Köster effect.²⁷

Heavily deformed metals, particularly aluminum, show another effect called the "viscosity" effect after the Köster effect has disappeared. A residual internal friction is observed provided that the measurements are made at sufficiently high temperatures or low frequencies. Fig. 21 shows the internal friction of heavily worked aluminum after a series of anneals at the temperatures indicated in the figure. The most complete study of this effect is that of Ké²⁸ and Zener and Ké²⁸ in which low frequency (torsional pendulum) and static measurements (relaxation) were made. These curves show that the internal friction keeps on rising with temperature and shows no relaxation effect. At the recrystallization

²⁷ A. S. Nowick, Internal Friction and Dynamic Modulus of Cold Worked Metals, *J. Appl. Phys.*, **25**, pp. 1129-1134, Sept., 1954.

²⁸ T. S. Ké, *Trans. A.I.M.E.*, **188**, p. 575, 1950 and T. S. Ké and C. Zener, Symposium on the Plastic Deformation of Crystalline Solids, U. S. Office of Naval Research, Pittsburgh, 1950.

temperature, 300°C, this effect disappears and the normal grain boundary relaxation returns. This effect is not observable in brass or iron at these temperatures since the lower melting temperature of aluminum gives it a much lower activation energy.

While sufficient data for the Köster effect has not been obtained to make certain any interpretation in terms of dislocation theory, two possibilities may be mentioned. When the material is highly worked, large numbers of new dislocations are produced principally along slip bands in the interior of the crystal grains. From the absence of a temperature dependence of the Köster effect they must be of the zigzag types²⁹ which run across minimum energy positions, such as those illustrated in Fig. 5, in a zigzag manner as shown in Fig. 22. Such dislocations

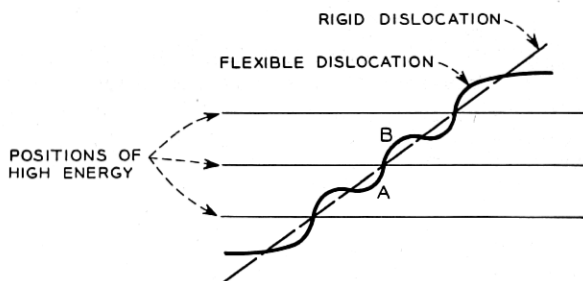


Fig. 22 — Form of zigzag dislocation that crosses lattice rows in a slip plane (after Cottrell).

are not bound by potential wells and their frequency of vibration is determined by their tension rather than by the limiting shearing stress for a potential well which was discussed in the first section. The equation for a stretched dislocation, as discussed by Koehler,¹³ can be written in the form

$$m \frac{\partial^2 x}{\partial t^2} + B \frac{\partial x}{\partial t} - \frac{T}{\pi} \frac{\partial^2 x}{\partial y^2} = T_{13} b \quad (74)$$

where m , the mass per unit length, is $\pi \rho b^2$; B is a dissipation constant, T is the tension of the dislocation equal to μb^2 , x is the displacement of the dislocation at a distance y from one end, and T_{13} the applied shearing stress. The natural frequency for a vibration loop is obtained by setting B and T_{13} equal to zero. The preferred shape of a vibration is then

$$x = A(y\ell - y^2) \quad (75)$$

²⁹ For a discussion of zigzag dislocations, see A. H. Cottrell, *Dislocations and Plastic Flow in Crystals*, p. 65, Oxford University Press, 1953.

which represents a zero displacement at $y = 0$ and $y = \ell$ with a parabolic shape in between. The average displacement for the dislocation is

$$\bar{x} = \frac{A}{\ell} \int_0^\ell (y\ell - y^2) dy = \frac{A\ell^2}{6} \quad (76)$$

Inserting this value in (74) and introducing the value $\partial^2/\partial t^2 = -\omega^2$, we have

$$\frac{\omega^2(\pi\rho b^2\ell^2)}{6} = \frac{2\mu b^2}{\pi} \quad (77)$$

Solving for the frequency we find

$$f = \frac{1}{2\pi\ell} \sqrt{\frac{12}{\pi^2} \frac{\mu}{\rho}} \quad (78)$$

When the zigzag dislocations are originally formed, some of them are probably relatively free from entanglement with other dislocations or with impurity atoms. In the course of time they gravitate towards other dislocations or atoms and form pinning points with them, thereby restricting their possible motion and the associated dissipation.

While they are free to vibrate, one possible cause of loss is the damped vibrations of the dislocations discussed by Koehler.¹³ Koehler considers that the dislocations can be made to follow the applied stress and due to the damping constant B of (74) abstract energy from the vibration. To a first approximation, the loss caused by this mechanism is proportional to the first power of the frequency and the fourth power of the loop length.¹³ Since no activation energy is involved, this loss should be independent of the temperature. As the loop length becomes smaller due to an increased number of pinning points, this loss rapidly decreases.

If the Köster loss is independent of the frequency, another possibility may be the thermal type of hysteresis loss, i.e., loss independent of frequency. For the case of free dislocations it is supposed that they can move in loops but the pinning points are not fixed points. Hence, energy abstracted from the mechanical vibration by the motion of the loop will not be coherent and therefore will not be returnable to the vibration. The loss calculated from such a mechanism will be

$$Q^{-1} = \frac{\pi b^2 \rho \ell f N_0 V_s}{\pi \sqrt{\mu \rho}} \quad (79)$$

Inserting f from (78) we find

$$Q^{-1} = \frac{\sqrt{3} b^2 N_0 V_s}{\pi^2} \quad (80)$$

where N_0 is the total number of loops present in the unpinned dislocations. This should be independent of the temperature at the time of forming. As these free dislocations gradually become pinned by other dislocations or atoms, the number, N_0 , decreases and the attenuation decreases while the value of Young's modulus increases, since the degree of displacement diminishes as the loops become pinned. Since $b \doteq 2.5 \times 10^{-8}$; $V_s \doteq 3.2 \times 10^5$ cm/sec for iron, Q^{-1} should be multiplied by 1.2 to transform from a Young's modulus strain along the axis to a shearing strain in the glide plane. Hence N_0 should have a value of

$$N_0 \doteq 1.3 \times 10^7 \quad (81)$$

Some idea of the effect of such a model on the elastic constants can be obtained by calculating the ratio of the plastic to elastic shear for a static force. From equations (74) and (76) the average displacement \bar{x} of a dislocation loop is

$$\bar{x} = \frac{\pi T_{13} \ell^2}{12\mu b} \quad (82)$$

The total plastic strain, due to the displacement of N_0 loops, is then

$$S_{13}^P = N_0 S b = N_0 \bar{x} \ell b = N_0 \frac{\pi T_{13} \ell^3}{12\mu} \quad (83)$$

where S is the average area of a loop. To this we add the elastic strain so that

$$\frac{S_{13}^P + S_{13}^E}{T_{13}} = \frac{1}{\mu^E} + \frac{\pi N_0 \ell^3}{12\mu} = \frac{1}{\mu} \quad (84)$$

Hence the difference between two constants is

$$\frac{\mu^E - \mu}{\mu\mu^E} \doteq \frac{\Delta\mu}{\mu\mu^E} = \frac{\pi N_0 \ell^3}{12\mu} \quad \text{or} \quad \frac{\Delta\mu}{\mu} = \frac{\pi N_0 \ell^3 \mu^E}{12\mu} \quad (85)$$

Using (46) to relate the change in elastic constant along the glide plane to the change in the elastic constant Y_0 for an isotropic material, we multiply the change in elastic constant of Fig. 20 by a factor of 1.2. Hence

$$\frac{\Delta\mu}{\mu} = 1.2 \times 0.01 \doteq \frac{\pi N_0 \ell^3}{12} \quad (86)$$

Since

$$b = 2.5 \times 10^{-8} \text{ cm} \quad (87)$$

we find

$$N_0 \ell^3 = 0.046; \quad \ell \doteq 1.5 \times 10^{-3} \text{ cm} \quad (88)$$

where we have used the value of $N_0 = 1.3 \times 10^7$. This appears to be a possible value for a free dislocation loop not pinned down by other dislocations. According to Nowick²⁷ the permanent change in the elastic modulus for heavily worked material, which does not recover below the recrystallization temperature, stems from the lowering of the true Young's modulus due to the decrease in the average interatomic force constants resulting from the deformation.

As soon as the free dislocations become tied down by other dislocations, this source of dissipation and modulus change disappears. As shown in Fig. 21, however, there remains another source of dissipation which appears to be related to the temperature actuated hysteresis effect previously discussed. If we take the difference between the actual attenuation curves and the grain boundary relaxation effect, which should always be present, the added attenuation can be represented by the equation

$$Q^{-1} = C e^{-(10,500/RT)} \quad (89)$$

where the constant C varies from

$$C = 2.0 \times 10^4 \text{ to zero} \quad (90)$$

as the annealing temperature goes from 125°C to the recrystallization temperature. Since this effect does not reach a peak value in the manner of the grain boundary relaxation effect, this cannot be a relaxation effect.

The mechanism considered here is that it is a temperature actuated hysteresis effect similar to that discussed previously except that the dislocations are not in a potential well and are bound by other dislocations rather than by impurity atoms. It is known that under conditions of severe deformations, each crystallite is broken into sub-grains by the production of slip bands. Hence the dislocations are present in these bands and in the course of time join into a network of dislocation loops. The slip bands are under a shearing stress equal to the limiting shearing stress of the crystal and under these conditions the data of Fig. 19 show that the activation energy for diffusion can be lowered to 10.5 kilocalories per mole. Hence the loss considered here is that due to thermal energy abstracted from the mechanical vibration by the incoherent energy of unpinned dislocation loops.

From (80) it is readily seen that the form of the loss equation should

be

$$Q^{-1} = \frac{\sqrt{3}b^2 V_a N_0 e^{-(10,500/RT)}}{\pi^2} \quad (91)$$

From the value of C in (90), the number of loops per cubic centimeter should be

$$N_0 \doteq 10^{15} \quad (92)$$

If we consider that the dislocations outline the form of an approximately regular mosaic structure, with $N_0 \ell^3 \doteq 1$; $\ell \doteq 10^{-5}$ cm; we find

$$N_0 \ell \doteq 10^{10} \text{ dislocations per sq cm} \quad (93)$$

which is a reasonable value for a hard worked material. In all probability, the dislocations concentrate in the slip bands and have a considerably higher density and smaller average loop length than given by (93). This type of loss does not show up in the same temperature range for brass and iron, as found by Köster, since the activation energy for these materials cannot be reduced to such a low value as for aluminum.